Comprehensive kinetics of electrochemically assisted ammonia removal in marine aquaculture recirculating systems

Alba Romano, Inmaculada Ortiz, Ane M. Urtiaga *

Department of Chemical and Biomolecular Engineering, University of Cantabria, Av. Los Castros 46, Santander 39005, Spain

ABSTRACT

This work reports a comprehensive kinetic analysis and modelling of the electrochemically assisted ammonia removal from marine aquaculture waters (RAS). The proposed model combines the kinetics of chlorine electrogeneration, experimentally determined, with the mechanism and kinetic parameters, taken from literature, of break point chlorination reactions involving aqueous chlorine (HClO and ClO$^-$), total ammonia nitrogen (TAN as NH$_3$ and NH$_4^+$), and the chlorinated derivatives of ammonia (monochloramine (NH$_2$C1), dichloramine (NHC1$_2$), and nitrogen trichloride (NC1$_3$)). The model has been validated with laboratory experiments, obtained in an electrochemical cell provided with Ti/RuO$_2$ anode and Ti cathode, and working with model sea water in the range of operating variables [TAN]$_0$ = 10–60 mg L^{-1} and j = 5 – 20 A m^{-2}; good agreement between simulated and experimental data for the progress of ammonia and combined chlorine concentrations assesses the validity and robustness of the kinetic model. Thus, this study provides the tools to analyse, predict and explain ammonia removal performance in the electrochemical treatment of marine RAS water.

1. Introduction

Intensive aquaculture is the fastest growing animal food-producing sector worldwide. Recirculating Aquaculture Systems (RAS) are land-based aquaculture facilities – either open air or indoors – that minimise water consumption by filtering, adjusting, and reusing the water [1]. RAS provides very high fish production per unit surface of land used but requires careful monitoring and regeneration of water, as its quality becomes altered due to feeding and metabolism of fish. Nitrogenous compounds (ammonia, nitrite and nitrate), organic matter and pathogens are generated, being ammonia nitrogen the most critical water quality parameter in fish culture.

In the most extended method of RAS water treatment, ammonia is mostly oxidized into nitrite and nitrate through nitrification in biological filters by means of *Nitrosomonas* and *Nitrobacter* bacteria [2]. However, the reduced performance of biofilters working with saline water has led to propose new alternatives to biological and physical-chemical processes such as, selective ion exchange, flocculation and membrane bioreactors [3–5]. Although relevant progress has been made in recent years, these technologies are not exempt of some drawbacks such as their high cost of operation, biological upsets, addition of chemical reagents, biofouling, or limited efficiency in dynamic

operation of RAS that make necessary, in several cases, additional water treatment [6].

Electrochemical oxidation has been identified as a promising alternative for water treatment in marine RAS aquaculture, promoting water and energy savings. Moreover, the electrolysis operating conditions can be easily controlled, facilitating adaptability of the technology to dynamic systems. Previous investigations have shown that in-situ chlorine electro-generation enables the almost complete removal of ammonia compounds [7,8].

The performance of electrooxidation processes is largely recognized to be strongly dependant on the anode material, because it determines the type of electrochemical oxidants that are generated in the treated waters [9] and influences the effectiveness of active chlorine generation [10]. For the indirect electrooxidation of ammonia through electrogenerated chlorine successful results have been previously reported working with different aqueous media using Boron Doped Diamond (BDD) [11,12] and RuO$_2$/Ti, a more cost-effective material that reported high yield of ammonia removal [13]. Anyway, the oxidation of total ammonia nitrogen (TAN) (NH$_4^+$/NH$_3$) occurs through the electrogeneration of chlorine (Cl$_2$), by direct oxidation of naturally occurring chloride on the anode, which is later hydrolysed to form hypochlorous acid (HClO/ClO$^-$), which reacts with TAN in a similar way to the breakpoint chlorination mechanism.

With regard to the kinetics of electrochemical TAN removal, although most works propose a second order reaction depending both on TAN and HClO concentration, there is no full agreement in literature. Dealing with chloride enriched wastewater, second order kinetics have been reported by Anglada et. al. [14] in the treatment of saline industrial effluents, and by Cabeza et al. [15] treating leachates from a municipal solid waste landfill site, with BDD anodic material in both studies. Díaz et al. [6] and Ruan et al. [16] reported second order kinetics in the treatment of marine aquaculture waters, using BDD and RuO_2-IrO_2/Ti as anode material, respectively. However, working with different aqueous systems, first order kinetics have been reported for ammonia removal; this is the case of Chen et al. [17] working with RuO_2–IrO_2–TiO_2/Ti as anode and titanium as cathode, and Ding et al. [18], working with graphite felt as cathode material and a dimensionally stable (DSA) anode with an IrO_2-RuO_2 coating. Furthermore, Li and Liu [19] reported zero-th order kinetics using stainless steel as cathode material and RuO_2/Ti and IrO_2/Ti as anode materials. Apart from the electrode materials, the configuration and dimensions of the electrochemical reactor and the characteristics of the electrolyte differed in most of the works.

In this work, a mechanistic kinetic model of TAN indirect electrooxidation in saline water is developed. The model integrates the kinetics of chlorine electrogeneration, which were experimentally determined in the present work, with breakpoint chlorination reactions whose kinetic expressions had been previously reported. The developed model has been validated through the comparison of simulated and experimental results of the progress of ammonia and combined chlorine concentration that were obtained in an electrochemical cell provided with RuO_2/Ti anode and Ti cathode and working with model sea water in the range of operation variables $[TAN]_0 = 10$–60 mg L^{-1} and $j = 5 - 20$ A m^{-2}. Based on the reliability of the reported model, this work will help to a better design, performance, and control of large-scale electrochemical water treatment for marines RAS systems.

2. Theoretical background

As above mentioned, the anodic oxidation of chloride in marine water can be represented by Eq. (1). Other reactions include hydrolysis of dissolved chlorine (Eq. (2)) and the acid dissociation of hypochlorous acid (Eq. (3)).

$$2Cl^- \rightarrow Cl_2(g) + 2e^- \tag{1}$$

$$Cl_2(g) + H_2O \leftrightarrow HClO + H^+ + Cl^- \tag{2}$$

$$HClO \leftrightarrow ClO^- + H^+ \tag{3}$$

The relative concentrations of Cl_2, HClO and ClO^- depend on the pH of the solution: Cl_2 prevails at very low pH, HClO in moderate acidic conditions and ClO^- in basic conditions. The sum of Cl_2, HClO and ClO^- will be denoted as free chlorine.

Electrogenerated chlorine oxidizes ammonia in the aqueous solution to form nitrogen through a series of intermediate reactions that involve the formation and conversion of mono-, di- and trichloramine. The mechanism and kinetics of ammonia breakpoint chlorination has been largely studied, in many cases in the context of chlorine mediated water disinfection processes. Table 1 details the most generalized reaction mechanism and rate expressions for ammonia chlorination reactions involving aqueous chlorine (HClO and ClO^-), aqueous ammonia (NH_3 and NH_4^+), and the chlorinated derivatives of ammonia: monochloramine (NH_2Cl), dichloramine ($NHCl_2$), and nitrogen trichloride (NCl_3). The sum of mono-, di- and trichloramine will be denoted as combined chlorine. This mechanism describes well the slow oxidation rate of ammonia in aqueous chloramine solution with Cl/N ratio <1 and the transition region of $1<$ Cl/N <1.6.

The kinetic model includes reactions which can be classified into: 1) Substitution reactions involving HClO and ammonia or the chlorinated derivatives of ammonia, and the corresponding hydrolysis reactions: r1 and r2 that describe the formation and hydrolysis of NH_2Cl; reactions r3 and r4 result in $NHCl_2$ formation; reaction r11 involves the formation of NCl_3, while r15 describes NCl_3 hydrolysis. 2) r5, the disproportionation reaction of monochloramine that results in dichloramine formation, and the corresponding back reaction r6; reaction r5 has been found to be generally acid catalysed. 3) The redox reactions that occur in the absence of measurable free chlorine and presence of free ammonia (r7, r8 and r9). 4) The redox reactions r12, r13 and r14 that occur when free chlorine is present. Reaction r10 was included by Leao et al. [20] to ensure a good fitting between experimental data and simulated data with the model.

The values of kinetic constants as collected from several references [21–25] are also detailed in Table 1. In particular, the model is capable of predicting the speciation and fate of chlorine containing oxidants over the transition region in which the chloride/nitrogen ratio is below the breakpoint chlorination Cl/N $> \approx 1.6$. More recently, results by other authors support the general perspective of the applied model [26,27].

3. Materials and Methods

Fig. 1 shows a schematic view of the experimental set-up [28]. An undivided electrochemical cell (ELOXlab RT-170, supplied by Apria Systems, Spain) was employed to carry out the experiments. The cell was provided with a Ti/RuO_2 anode and Ti cathode, each one with an effective area of 176 cm^2. The inter-electrode gap was set at 0.2 cm. The saline water stream circulated upwards along the closed rectangular channel, at a flowrate of 6.5 L min^{-1}, driven by a magnetic pump (MD-R, Iwaki). The model seawater solution was stored in the thermostatic feed tank with a volume of 2 L, working at 22°C. The experiments were performed in galvanostatic conditions using a power supply (Agilent 6654 A, maximum output of 9 A and 60 V), and the influence of the applied current density was studied in the range between 5 and 50 A m^{-2}.

Model seawater solutions were prepared using sodium chloride (Panreac, purity $\geq$ 99.5%) and deionized water. Sodium chloride concentration (28.4 g NaCl L^{-1}) was selected as representative of the conditions of a RAS production unit located at the northern coast of Spain. The average pH in the model seawater solution was 7. Ammonium chloride (Scharlau, purity $\geq$ 99.5%) was added as source of ammonia.

During the experiments, water samples were taken from the feed tank at fixed time intervals, using a syringe. The pH was monitored but not adjusted, using a Thermo Scientific Orion Star A325 pH meter, equipped with a specific electrode for seawater (Orion ROSS Triode pH/ATC electrode); water conductivity was measured with a Crison CM 35 conductivity meter, that was calibrated with standards in the range 147 μScm^{-1} – 12.88 mS cm^{-1}. The concentration of total ammonia nitrogen, nitrates and nitrites in solution was determined with a spectrophotometer (Spectroquant Prove 100, Merck) using commercial kits and according to Standard Methods: 4500-NH3-D, 4500-NO2-B, 4500-NO3, respectively [29]. The limit of quantification (LOQ) and limit of detection (LOD), as provided by the kits certificates (Merck), were: i) ammonia nitrogen: LOQ 0.05 mg $(NH_4^+ - N)$/L, LOD 0.009 mg/L; ii) nitrite nitrogen, LOQ 0.02 mg$(NO_2^- - N)$/L, LOD 0.002 mg/L; and iii) nitrate nitrogen, LOQ 0.2 mg$(NO_3^- - N)/L$, LOD: 0.04 mg/L. Free chlorine, combined chlorine and total chlorine concentrations were analysed using a portable visible colorimeter (HI 95734, Hanna Instruments Company), with Hanna commercial test kit (HI-93734-01 Chlorine, Free and Total HR, DPD Method, range of chlorine concetration 0.00 – 10 mg/L). The DPD method is based on the oxidation of N,*N*-diethyl-p-phenylenediamine by chlorine, that results in a colored compound, which is analyzed in a visible

Table 1
Breakpoint chlorination reactions and kinetic constants.

	Reaction	Rate expression	Rate constant (25 °C)	Ref.
r1	$HClO + NH_3 \rightarrow NH_2Cl + H_2O$	$k_1[HClO][NH_3]$	$k_1 = 1.78 \cdot 10^5\ mM^{-1}\ min^{-1}$	[22]
r2	$NH_2Cl + H_2O \rightarrow HClO + NH_3$	$k_2[NH_2Cl]$	$k_2 = 1.2 \cdot 10^{-3}\ min^{-1}$	[21]
r3	$HClO + NH_2Cl \rightarrow NHCl_2 + H_2O$	$k_3[HClO][NH_2Cl]$	$k_3 = 16.6\ mM^{-1}\ min^{-1}$	[23]
r4	$NHCl_2 + H_2O \rightarrow HClO + NH_2Cl$	$k_4[NHCl_2]$	$k_4 = 3.9 \cdot 10^{-5}\ min^{-1}$	[21]
r5	$NH_2Cl + NH_2Cl \rightarrow NHCl_2 + NH_3$	$k_5[NH_2Cl][NH_2Cl]$	$k_5 = 4.16 \times 10^{-1}[H^+]mM^{-1}\ min^{-1}$	[21]
r6	$NHCl_2 + NH_3 \rightarrow NH_2Cl + NH_2Cl$	$k_6[NHCl_2][NH_3][H^+]$	$k_6 = 3.66\ mM^{-2}\ min^{-1}$	[24]
r7	$NHCl_2 + H_2O \rightarrow NOH^a + P^b$	$k_7[NHCl_2][OH^-]$	$k_7 = 10.02\ mM^{-1}\ min^{-1}$	[24]
r8	$NHCl_2 + NOH \rightarrow HClO + P^b$	$k_8[NOH][NHCl_2]$	$k_8 = 1.67 \cdot 10^3\ mM^{-1}\ min^{-1}$	[21]
r9	$NH_2Cl + NOH \rightarrow P^b$	$k_9[NOH][NH_2Cl]$	$k_9 = 498\ mM^{-1}\ min^{-1}$	[21]
r10	$NH_2Cl + NHCl_2 \rightarrow P^b$	$k_{10}[NH_2Cl][NHCl_2]$	$k_{10} = 9.17 \cdot 10^{-4}\ mM^{-1}\ min^{-1}$	[21]
r11	$HClO + NHCl_2 \rightarrow NCl_3 + H_2O$	$k_{11}[HClO][NHCl_2]$	$k_{11} = 1.97 \times 10^5[OH^-] + 5.4[ClO^-]mM^{-1}min^{-1}$	[21]
r12	$NHCl_2 + NCl_3 + 2H_2O \rightarrow 2HClO + P^b$	$k_{12}[NHCl_2][NCl_3][OH^-]$	$k_{12} = 3.3 \cdot 10^6\ mM^{-2}\ min^{-1}$	[21]
r13	$NH_2Cl + NCl_3 + H_2O \rightarrow HClO + P^b$	$k_{13}[NH_2Cl][NCl_3][OH^-]$	$k_{13} = 8.3 \cdot 10^4\ mM^{-2}\ min^{-1}$	[21]
r14	$NHCl_2 + 2HClO + H_2O \rightarrow NO_3^- + 5H^+ + 4Cl^-$	$k_{14}[NHCl_2][ClO^-]$	$k_{14} = 13.86\ mM^{-1}\ min^{-1}$	[21]
r15	$NCl_3 + H_2O \rightarrow HClO + NHCl_2$	$k_{15}[NCl_3]$	$k_{15} = 9.6 \times 10^{-5} + 4.8 \times 10^{-1}[OH^-] + 5.34 \times 10^{-2}[OH^-]^2,\ min^{-1}$	[25]

[a] NOH: assumed formula for the unidentified intermediate.
[b] P: products may include N_2, H_2O, Cl^-, H^+, NO_3^-.
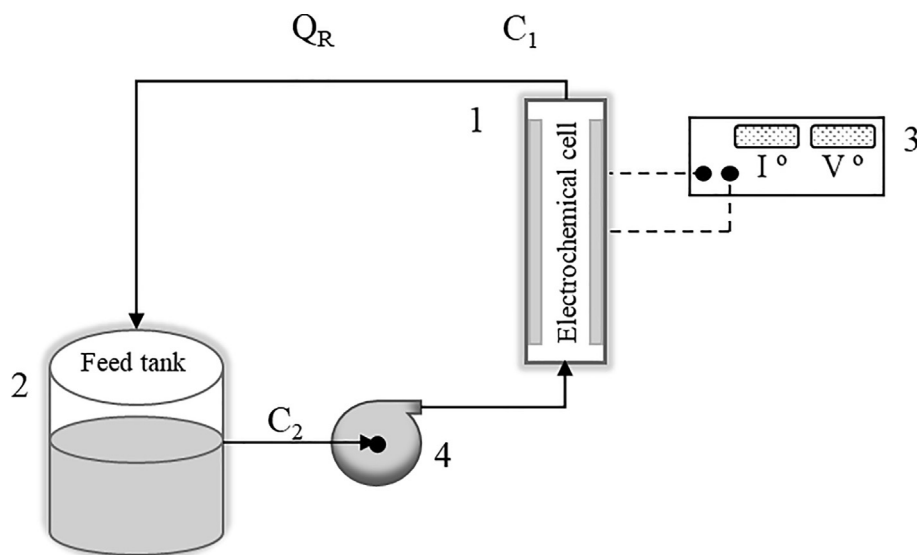
Fig. 1. Schematic diagram of the experimental system: 1. Electrochemical cell; 2. Feed tank; 3. DC power supply; 4. Pump. C_1, C_2 and Q_R are concentration and flowrate variables used in the kinetic model presented in section 5.

spectrophotometer. The kit is an adaptation of the Standard Methods 4500-Cl G. The chlorine analysis resulting from the kit is expressed as mg Cl_2/L. Considering that at the solution pH, free chlorine is in the form of $HClO/ClO^-$ (see reactions (1-3)), we converted the Cl_2 concentration to free chlorine concentration in a mol by mol basis.

4. Results

4.1. Influence of the current density in the kinetics of chlorine electro-generation

Initially, batch electrolysis experiments were performed at several current densities: from 5 to 50 A m $^{-2}$, in absence of ammonia, to determine the kinetics of active chlorine formation as a function of the current density. To that end, samples were taken from the recirculation tank at fixed time intervals, and free chlorine was analysed; results are depicted in Fig. 2.

During the electrolysis of seawater, electro-generated chlorine ($Cl_{2\ (g)}$ in Eq. (1)) is hydrolysed to form hypochlorous acid (Eq. (2)), which at seawater pH is dissociated to form a mixture of $HClO/ClO^-$ (Eq.

(3)), a mixture referred to as free available chlorine. In this set of experiments, the initial water pH was around 7.7, and during seawater electrolysis, it became slightly alkaline, with values rising up to 8.5. The pH evolution can be explained by the cathodic conversion of protons into hydrogen.

Fig. 2 shows that at any current density, the chlorine concentration increased linearly with time. The linear kinetics can be explained by the excess of chloride reactant in the highly saline model seawater. It was checked (data not shown) that in the course of the experimental time the chloride concentration was almost constant at a value of 17 g L^{-1}. Increasing the applied current density enhanced the rate of chlorine electro-generation. The apparent kinetic constant of chlorine formation was obtained by the linear fitting of the experimental data in Fig. 2, according to the integration of the chlorine mass balance in the feed tank given by Eq. (4),

$$V \frac{d[HClO + ClO^-]}{dt} = V \frac{d[Cl_{2(g)}]}{dt} = \frac{\varphi Aj}{nF} \tag{4}$$

where $[HClO + ClO^-] = [Cl_{2(g)}]$ is the free chlorine concentration expressed as (mmol Cl_2 L^{-1}) measured in the feed tank; t is the
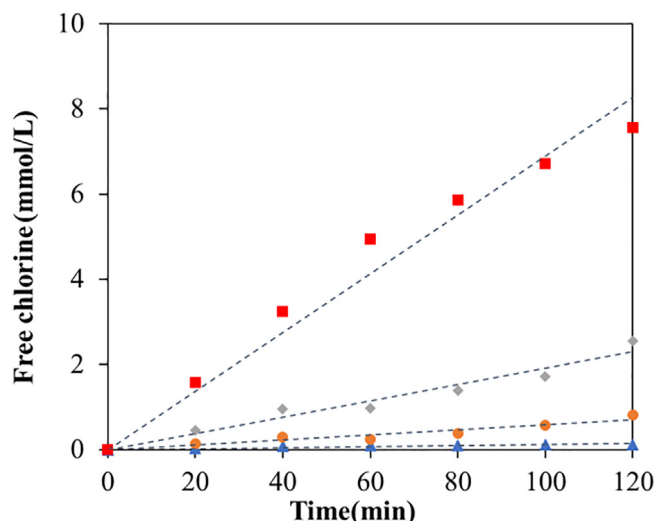
Fig. 2. Change of free chlorine concentration with time in the feed tank, as a function of the applied current density. ▲ j = 5 A m^{-2}; ● j = 10 A m^{-2}; ◆ j = 20 A m^{-2}; ■ j = 50 A m^{-2}. Model seawater in absence of ammonia. Dotted lines correspond to the linear fitting of experimental data. The background electrolyte is model seawater, NaCl 28 g L^{-1}. Initial pH = 7.7.

electrolysis time (min); n is the number of electrons transferred in the reaction (n = 2); F is the Faraday constant (96485 C mol^{-1}); V is the volume of the electrolyte solution (V = 2 L); A is the anode area (A = 175 cm^2); j is the applied current density (A m^{-2}); φ is the current efficiency of anodic chlorine production (%). After fitting the experimental data of free chlorine concentration to Eq. (4), the current efficiency φ for chlorine production in this experimental system was calculated to be 33%. Similar trends were reported in a previous study that used seawater as electrolyte for active chlorine generation in the electrochemical cell formed by a Ti cathode and an IrO$_2$–RuO$_2$/Ti anode, with pH and temperature not adjusted [30].

4.2. Indirect ammonia electro-oxidation

Next, the electrochemically assisted oxidation of ammonia contained in model seawater was experimentally analysed. During the electrolysis of seawater containing ammonia, the electrogenerated chlorine reacts with ammonia to form nitrogen gas, through intermediate reactions that involve the formation and conversion of chloramines, as Table 1 details. Fig. 3a shows the results of ammonia removal in

the experiments performed at 10 A m^{-2}, and for initial ammonium concentrations of 0.55, 1.1, 2.2 and 3.3 mmol N L^{-1}, respectively (equivalent to 10, 20, 40 and 60 mg NH$_4^+$ L^{-1}). In all experiments, the change in TAN concentration with time presents a quasi-linear trend. The slopes of the linear fitting of TAN concentration vs. time for these experiments are −0.46, −0.40, −0.40, −0.39 mmol N L^{-1}h^{-1} with correlation coefficients (r^2) of 0.97, 0.99, 0.94 and 0.98, respectively. The pH was continuously monitored but not adjusted. As result of the reactions that take place during TAN oxidation (reactions r7, r8, r9, r10, r11, r13, r14 and r15) the pH dropped gradually from an average value of 7.5 to 4.5, although it returned to neutrality after complete ammonia removal.

Fig. 3b depicts the ammonia concentration decrease with time for the three values of current density analysed, 5, 10 and 20 A m^{-2}, working with initial ammonia concentration 0.55 mmol N L^{-1}. The data fit adequately to linear trends mostly due to the fact that the rate of ammonia oxidation is dominated by chlorine generation, whose electrogeneration rate follows a zero-th order trend (strongly influenced by the current density, as it is shown in Eq. (4)). During ammonia oxidation the concentration of free chlorine was maintained at very low values.

The kinetic data depicted in Fig. 3 should be described after integration of the rate of the reactions scheme contained in Table 1. Furthermore, Fig. 2 shows that the increase in the applied current density enhances the rate of chlorine-formation, which in turn, makes a positive contribution to the rate of the main reactions between ammonia and combined chlorine. This result therefore, explains the reason why increasing the current density accelerates the kinetics of ammonia removal. After the analysis of the kinetic data and the influence of the main operation variables on the rate of ammonia oxidation, next, the kinetic modelling is reported.

5. Kinetic model implementation

The kinetic model to describe the indirect electrooxidation of ammonia will contain electrochemical parameters obtained in the chlorine electrogeneration experiments (Fig. 2) together with kinetic equations and parameters reported in literature for breakpoint chlorination reactions involved in the ammonia oxidation mechanism, that are collected in Table 1. Then, simulated data with the kinetic model will be validated with data obtained in the electrochemically assisted ammonia removal experiments.

The aim of the proposed model is to describe the evolution over time of TAN and combined chlorine concentration during the RAS water treatment, as a function of operating variables. This model divides the electrochemical process in two main zones:
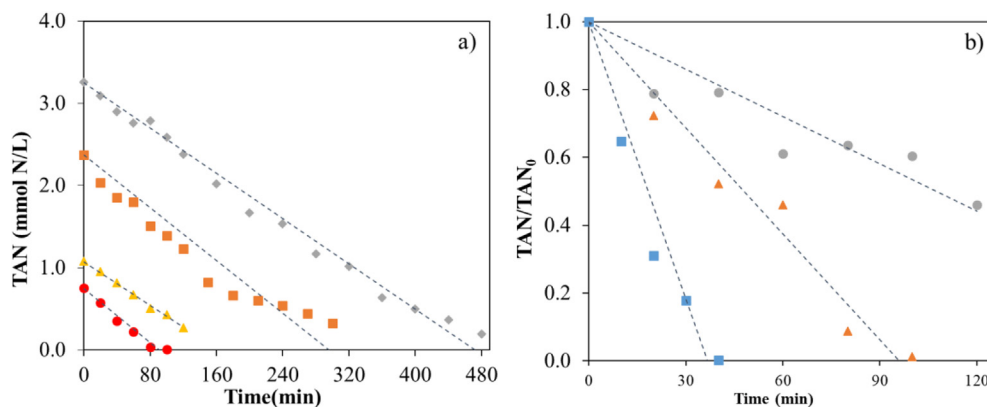

Fig. 3. a) Influence of the initial ammonia concentration on TAN removal, at j = 10 A m^{-2} and ● [TAN]$_0$ = 0.55 mmol L^{-1}, ▲ [TAN]$_0$ = 1.1 mmol L^{-1}, ■ [TAN]$_0$ = 2.2 mmol L^{-1}, ◆[TAN]$_0$ = 3.3 mmol L^{-1}. b) Influence of current density in TAN removal, at [TAN]$_0$ = 0.60 ± 0.08 mmol L^{-1} and ● j = 5 A m^{-2}, ▲ j = 10 A m^{-2}, ■ j = 20 A m^{-2}. The background electrolyte is model seawater, NaCl 28 g L^{-1}. Initial pH = 7.5.

electrochemical cell and feed tank as detailed in the experimental section. The following assumptions will be considered for integrating the mass balances:

- The concentration of any species at the outlet of the electrochemical cell and at the inlet of the feed tank is the same, resulting in the following additional equations for any species,

$$C_{out,cell} = C_{in,tank} = C_1 \tag{5}$$

$$C_{out,tank} = C_{in,cell} = C_2 \tag{6}$$

- Uniform mixing in the cell and in the feed tank
- Breakpoint chlorination reactions take place in both the electrochemical cell and feed tank sections; chlorine generation occurs only in the electrochemical cell section.

- In the fitting of experimental data to the kinetic model, NOH concentration (unidentified monochloramine auto decomposition intermediate species) during electro-oxidation process is calculated to be $2 \cdot 10^{-4}$ mmol L^{-1}.
- TAN electro-oxidation results in increasing acidity and decreasing pH down to pH = 4.5 when TAN has been completely removed (corroborated experimentally).

To describe the kinetics of the indirect TAN electrooxidation process, we consider the mass balances of the following species: TAN, HClO, NH$_2$Cl, NHCl$_2$, NCl$_3$, NOH and NO$_3^-$. The mass balance to each species considers the reactions in which each species participates and their respective kinetic expressions r_x collected in Table 1, as follows,

- In the electrochemical cell,

$$V_{cell} \cdot \frac{d_{Iy}}{d} = Q_R \cdot C_{2y} - Q_R \cdot + \sum_{r_1}^{r_{15}} V_{cell} \cdot r_x \tag{7}$$
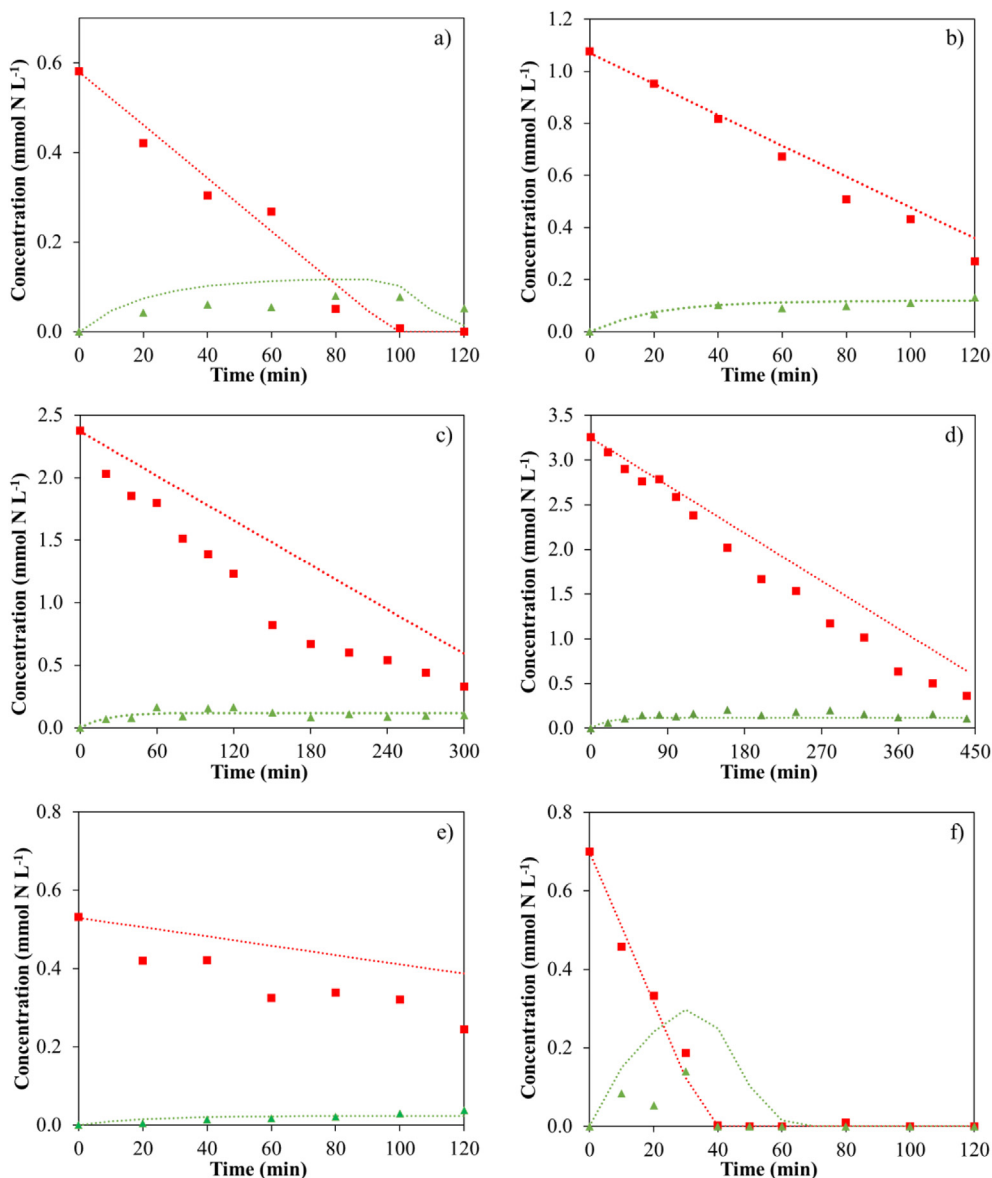

Fig. 4. Experimental data (symbols) and simulated values (dotted lines) of TAN (■) and combined chlorine (▲) concentration in the recirculating feed tank, operating the electrochemical systems at different initial ammonia concentration and current density. a) [TAN]$_0$ = 0.55 mmol L^{-1}, j = 10 A m^{-2}; b) [TAN]$_0$ = 1.1 mmol L^{-1}, j = 10 A m^{-2}; c) [TAN]$_0$ = 2.2 mmol L^{-1}, j = 10 A m^{-2}; d) [TAN]$_0$ = 3.3 mmol L^{-1}, j = 10 A m^{-2}; e) [TAN]$_0$ = 0.53 mmol L^{-1}, j = 5 A m^{-2}; f) [TAN]$_0$ = 0.70 mmol L^{-1}, j = 20 A m^{-2}.

- In the feed tank,

$$V_{tank} \cdot \frac{d}{d} = Q_R \cdot C_{1y} - Q_R \cdot C_{2y} + \sum_{r_1}^{r_{15}} V_{tank} \cdot r_x \qquad (8)$$

where V_{cell} and V_{tank} are the volume (L) of the cell and feed tank respectively, C_{1y} and C_{2y} are the molar concentration (mmol L^{-1}) of species y in the electrochemical cell and in the feed tank, respectively and Q_R is the recirculating flow rate (L min^{-1}). The third term in both mass balances refers to the sum of all the rate expressions where the considered species is involved, and r_x is the rate expression (mmol $L^{-1} min^{-1}$) of a defined reaction as depicted in Table 1, taken with positive value when it refers to the generation rate and with negative value for consumption reactions.

When Eqs. (7 and 8) are applied to free chlorine (HClO), the chlorine electro-generation kinetic parameter is included in the cell mass balance. Considering the experimental analysis presented in the previous section 4.2, the rate of chlorine electro-generation was considered zero-th order, described as follows,

$$\frac{dC_{HClO}}{dt} = r_{HClO} = k_{HClO} \qquad (9)$$

where k_{HClO} is the kinetic constant of chlorine electrogeneration (mmol L^{-1} min^{-1}) at 22 °C and depends on the applied current density (A m^{-2}).

The kinetic model for free chlorine (HClO) electro-generation in absence of TAN, describes two main zones of the experimental system as follows,

- Electrochemical cell,

$$V_{cell} \cdot \frac{d_{1HClO}}{d} = Q_R \cdot C_{2HClO} - Q_R \cdot {}_{1HClO} + V_{cell} \cdot k_{HClO} \qquad (11)$$

- Feed tank,

$$V_{tank} \cdot \frac{d}{d} = Q_R \cdot C_{2HClO} - Q_R \cdot C_{1HClO} \qquad (12)$$

The kinetic constant of free chlorine generation (k_{HClO}) was estimated using the Aspen Custon modeler V10s tool. The estimation algorithm used the weighted least squares minimization criterion as given in Eq. (13),

$$min \left\{ \sum_{n=1}^{N} \sum_{i=1}^{I} \left(y_{exp,i} - y_i \right)^2 \right\} \qquad (13)$$

where $y_{exp,i}$ (mmol L^{-1}) is the experimental chlorine concentration, obtained from the experiments of chlorine electro-generation in absence of TAN (Fig. 2), y_i (mmol L^{-1}) is the calculated chlorine concentration by the model, N is the number of experiments performed at the same current density. The estimated values of k_{HClO} were 0.069, 0.343 and 1.11 mmol L^{-1} min^{-1} at applied current densities of 5, 10 and 20 A m^{-2} respectively.

To corroborate the model accuracy in the prediction of ammonia removal by means of seawater electrochlorination, simulated data of TAN and combined chlorine concentration are plotted in Fig. 4 for several values of current density and initial ammonia concentration. Satisfactory correlation between experimental and model results is observed in Fig. 4. Thus, it can be concluded that the mathematical model, that describes the influence of the applied current density and initial TAN concentration, is a very useful tool for the design and optimization of TAN removal through indirect electro-oxidation besides, the model accounts for combined chlorine prediction, which ultimately can be used as tool for controlling residual chloramines content in RAS water.

6. Conclusions

This work reports the kinetic analysis and modelling of chlorine electrogeneration and simultaneous ammonia chlorination in model seawater that simulates process water in marine RAS aquaculture systems. The kinetic experimental analysis of free chlorine generation in the electrochemical cell provided with Ti/RuO2 anodes revealed that chlorine electrogeneration was strongly dependent on the applied current density, showing zero-th order rate with kinetic parameter for active chlorine generation k_{HOCl} ranging from 0.069 to 1.11 mmol L^{-1} min^{-1} for increasing j between 5 and 20 A m^{-2}.

Ammonia removal took place in the bulk aqueous phase of both the electrochemical reactor and the recirculating water tank through chlorination reactions involving free chlorine, ammonia, and combined chlorine species (monochloramine, dichloramine, and nitrogen trichloride). From the results obtained it is confirmed that the electrochemically assisted chlorination is an effective method for the removal of total ammonia nitrogen in process water of the marine aquaculture sector. The experimental analysis showed the strong dependency of ammonia removal rate on the applied current density, and the combined influence of ammonia initial content in the low concentration range between 10 and 60 mg L^{-1} of interest in the treatment of RAS water.

The reported process model describes ammonia and chloramines evolution by combining the kinetics of chlorine electrogeneration and the reactions mechanism between ammonia and chlorine in aqueous media, that considers a reactions scheme describing the combined region (0< Cl/N ≤ 1), the transition region (1< Cl/N ≤ 1.5) and the breakpoint region (Cl/N >1.5). The good agreement between simulated values and experimental results of ammonia nitrogen and combined chlorine confirm the robustness of the proposed model. Thus, the reported model advances the state-of-the-art knowledge on the mechanistic kinetics of TAN indirect electrooxidation and constitutes a very useful tool for the design and control of TAN and combined chlorine concentration in the electrochemical treatment of RAS waters.

CRediT authorship contribution statement

Alba Romano: Methodology, Investigation, Writing – original draft. **Inmaculada Ortiz:** Conceptualization, Writing – review & editing, Supervision. **Ane M. Urtiaga:** Conceptualization, Writing – review & editing, Funding acquisition.

Declaration of Competing Interest

The authors declare that they have no known competing financial interests or personal relationships that could have appeared to influence the work reported in this paper.

Acknowledgments

References

[1] EUFOMA European Market Observatory for Fisheries and Aquaculture Products. 2020. Recirculating Aquaculture Systems. Publications Office of the European Union. Brussels.
[2] J. Davidson, N. Helwig, S.T. Summerfelt, Fluidized sand biofilters used to remove ammonia, biochemical oxygen demand, total coliform bacteria, and suspended solids from an intensive aquaculture effluent, Aquac. Eng. 39 (1) (2008) 6–15, https://doi.org/10.1016/j.aquaeng.2008.04.002.

[3] J.M. Ebeling, K.L. Rishel, P.L. Sibrell, Screening and evaluation of polymers as flocculation aids for the treatment of aquacultural effluents, Aquac. Eng. 33 (4) (2005) 235–249, https://doi.org/10.1016/j.aquaeng.2005.02.001.

[4] N. Miladinovic, L.R. Weatherley, Intensification of ammonia removal in a combined ion-exchange and nitrification column, Chem. Eng. J. 135 (1-2) (2008) 15–24, https://doi.org/10.1016/j.cej.2007.02.030.

[5] T. Pulefou, V. Jegatheesan, C. Steicke, S.-H. Kim, Application of submerged membrane bioreactor for aquaculture effluent reuse, Desalination 221 (1-3) (2008) 534–542, https://doi.org/10.1016/j.desal.2007.01.114.

[6] V. Díaz, R. Ibáñez, P. Gómez, A.M. Urtiaga, I. Ortiz, Kinetics of nitrogen compounds in a commercial marine Recirculating Aquaculture System, Aquac. Eng. 50 (2012) 20–27, https://doi.org/10.1016/j.aquaeng.2012.03.004.

[7] V. Díaz, R. Ibáñez, P. Gómez, A.M. Urtiaga, I. Ortiz, Kinetics of electro-oxidation of ammonia-N, nitrites and COD from a recirculating aquaculture saline water system using BDD anodes, Water Res. 45 (1) (2011) 125–134, https://doi.org/10.1016/j.watres.2010.08.020.

[8] A. Romano, A.M. Urtiaga, I. Ortiz, Optimized energy consumption in electrochemical-based regeneration of RAS water, Sep. & Purif. Technol. 240 (2020) 116638, https://doi.org/10.1016/j.seppur.2020.116638.

[9] E. Lacasa, J. Llanos, P. Cañizares, M.A. Rodrigo, Electrochemical denitrificacion with chlorides using DSA and BDD anodes, Chem. Eng. J. 184 (2012) 66–71, https://doi.org/10.1016/j.cej.2011.12.090.

[10] J. Jeong, C. Kim, J. Yoon, The effect of electrode material on the generation of oxidants and microbial inactivation in the electrochemical disinfection processes, Water Res. 43 (4) (2009) 895–901, https://doi.org/10.1016/j.watres.2008.11.033.

[11] A. Anglada, R. Urtiaga, A. Urtiaga, I. Ortiz, Electrochemical oxidation of saline industrial wastewaters using boron-doped diamond anodes, Catal. Today 151 (1-2) (2010) 178–184, https://doi.org/10.1016/j.cattod.2010.01.033.

[12] G. Pérez, J. Saiz, R. Ibañez, A.M. Urtiaga, I. Ortiz, Assessment of the formation of inorganic oxidation by-products during the electrocatalytic treatment of ammonium from landfill leachates, Water Res. 46 (8) (2012) 2579–2590, https://doi.org/10.1016/j.watres.2012.02.015.

[13] Díaz, V., 2013. Regeneration and reuse of seawater in intensive aquaculture systems through the application of electro-oxidation. PhD Thesis. University of Cantabria. https://doi.org/MEE2011-0031.

[14] A. Anglada, A. Urtiaga, I. Ortiz, Pilot scale performance of the electro-oxidation of landfill leachate at boron-doped diamond anodes, Env. Sci. Technol. 43 (6) (2009) 2035–2040, https://doi.org/10.1021/es802748c.

[15] A. Cabeza, A.M. Urtiaga, I. Ortiz, Electrochemical Treatment of Landfill Leachates Using a Boron-Doped Diamond Anode, Ind. Eng. Chem. Res. 46 (5) (2007) 1439–1446, https://doi.org/10.1021/ie061373x.

[16] Y. Ruan, C. Lu, X. Guo, Y. Deng, S. Zhu, Electrochemical treatment of recirculating aquaculture wastewater using a Ti/RuO2-IrO2 anode for synergetic total ammonia nitrogen and nitrite removal and disinfection, Trans. ASABE 59 (2016) 1831–1840. https://doi.org/10.13031/trans.59.11630.

[17] J. Chen, H. Shi, J. Lu, Electrochemical treatment of ammonia in wastewater by RuO2-IrO2-TiO2/Ti electrodes, J. Appl. Electrochem. 37 (10) (2007) 1137–1144, https://doi.org/10.1007/s10800-007-9373-6.

[18] J. Ding, Q. Zhao, Y. Zhang, L. Wei, W. Li, K. Wang, The eAND process: Enabling simultaneous nitrogen-removal and disinfection for WWTP effluent, Water Res. 74 (2015) 122–131, https://doi.org/10.1016/J.WATRES.2015.02.005.

[19] L. Li, Y. Liu, Ammonia removal in electrochemical oxidation: Mechanism and pseudo-kinetics, J. Hazard. Mater. 161 (2-3) (2009) 1010–1016, https://doi.org/10.1016/j.jhazmat.2008.04.047.

[20] Leao, S.F. 1981. Kinetics of combined chlorine: reactions of substitution and redox. PhD Thesis. University of California; Berkeley, CA.

[21] C.T. Jafvert, R.L. Valentine, Reaction Scheme for the Chlorination of Ammoniacal Water, Environ. Sci. Technol. 26 (3) (1992) 577–586, https://doi.org/10.1021/es00027a022.

[22] Z. Qiang, C.D. Adams, Determination of Monochloramine Formation Rate Constants with Stopped-Flow Spectrophotometry, Environ. Sci. Technol. 38 (5) (2004) 1435–1444, https://doi.org/10.1021/es0347484.

[23] Morris, J.C., Isaac, R.A. 1983. Critical review of kinetic and thermodynamic constants for the aqueous chlorine-ammonia system., in: Water Chlorination: Environmental Impact and Health Effects. 49–62.

[24] V.C. Hand, D.W. Margerum, Kinetics and Mechanisms of the Decomposition of Dichloramine in Aqueous Solution, Inorg. Chem. 22 (10) (1983) 1449–1456, https://doi.org/10.1021/ic00152a007.

[25] K. Kumar, R.W. Shinness, D.W. Margerum, Kinetics and mechanisms of the base decomposition of nitrogen trichloride in aqueous solution, Inorganic Chemistry 26 (21) (1987) 3430–3434.

[26] Huang, X. 2008. Reactions between aqueous chlorine and ammonia: A predictive model. PhD Thesis Dissertation. Northeastern University, Boston.

[27] D. Trogolo, J.S. Arey, Equilibria and Speciation of Chloramines, Bromamines, and Bromochloramines in Water, Environ. Sci. Technol. 51 (1) (2017) 128–140, https://doi.org/10.1021/acs.est.6b0321910.1021/acs.est.6b03219.s001.

[28] Urtiaga, A., Fernández-Castro, Gómez, P., Ortiz, I. 2014. Remediation of wastewaters cotaining tetrahydrofurane. Study of the electrochemical mineralization on BDD electrodes. Chem. Eng. J. 239. 341-350. https://doi.org/10.1016/j.cej.2013.11.028

[29] APHA. Standard Methods for Examination of Water and Wastewater. 20th ed. American Public Health Association. Washington, DC. 20th ed. ed. American Public Health Association, Washington, DC. 1998.

[30] S. Yang, Z. Han, X. Pan, Z. Yan, J. Yu, Nitrogen oxide removal using seawater electrolysis in an undivided cell for ocean-going vessels, RSC Adv. 6 (115) (2016) 114623–114631, https://doi.org/10.1039/C6RA24537D.